

Part II: *Ab Initio* and NMR Investigations into the Barrier to Internal Rotation of various Oxo- and Thio- Analogues of 2-Oxo-2*H*-chromen-7-yl Dimethylcarbamates

Caryl K.A. Janse van Rensburg, Ross S. Robinson* and Hendrik G. Kruger

Warren Research Laboratory, School of Chemistry, University of KwaZulu-Natal,
Private Bag X01, Scottsville, Pietermaritzburg, 3209 South Africa.

Received 13 December 2010, revised 15 February 2011, accepted 20 June 2011.

Submitted by invitation to celebrate 2011 the 'International Year of Chemistry'.

ABSTRACT

A range of 2-oxo-2*H*-chromen-7-yl dimethylcarbamates were synthesized as described in part I of this publication, containing either an oxygen or sulphur α to the carbonyl or thiocarbonyl group of the amide moiety. Variable temperature and exchange spectroscopy NMR was performed on these compounds and the barrier to free amide rotation was calculated. Each of these compounds were also modelled *ab initio* and the gas phase barrier to rotation calculated. These three sets of data were compared and the influence of the α -heteroatom on rotation for amides and thioamides evaluated.

KEYWORDS

Thiocarbonyl, amide, rotational barrier.

1. Introduction

The barrier to internal rotation in amides and thioamides has been the subject of much attention¹ over past years due to the importance of the amide bond in proteins (and peptides), the secondary and tertiary structure thereof and thus their biological activity.^{2–4} In the application of peptide design and elucidation of the structure–activity relationships thereof, it is crucial to understand the conformational properties of such amide bonds.⁵ Similarly carbamates have gained importance in peptide chemistry as a protecting strategy for the amine groups of amino acid moieties.⁶ They also play an important function in the pharmaceutical, agricultural, and chemical industries, reiterating the importance in understanding the methods and influences of amide resonance.^{7–9} For like reasons, thiocarbamates and selenocarbamates are of equal importance.^{9–11}

The most widely used and generally accepted explanation for



Scheme 1

the hindered rotation is the classical model of chemical resonance as proposed by L. Pauling (1977)^{12,13} shown in Scheme 1.

Transfer of the nitrogen lone pair to the electron deficient carbonyl carbon results in delocalized π character along the N-C-O bonds. Accordingly, the C-N bond is stabilized by the above ionic configuration in planar amides by adopting partial double bond character.⁶ It has long been known that thioamides have a larger barrier to internal rotation than their amide analogues; however, according to Pauling's model, the lesser electronegativity of sulphur compared to oxygen predicts the

opposite effect (!).¹ For this reason, a new model has been put forward by Wiberg *et al.* that proposes electron transfer on rotation occurs in the direction of C \rightarrow N rather than O \rightarrow N as illustrated above.^{14–16} Because oxygen is more electronegative than carbon, it withdraws electron density to itself, polarizing the C=O bond in both the σ and π systems.¹⁷ This in turn allows the nitrogen lone pair to merge into a p orbital capable of interacting with the deficient carbon.¹⁷ *Ab initio* studies lead by Wiberg *et al.* on formamide revealed that the oxygen is effectively a spectator to the process of rotation away from planarity. Evidence for this is seen by examining both the bond lengths and charge distributions on the carbonyl and C-N bonds. On rotation from planarity, the length of the C-N bond increases by 0.08 Å where the C-O bond decreases only 0.01 Å,¹⁴ this indicates there is partial double bond character in the planar form originating from the C-N bond and the carbonyl is reasonably unaffected. This does not, however, explain why thioamides have a larger rotational barrier than amides. *Ab initio* studies have shown that amide resonance, and thus the magnitude of the barrier, increases as the electronegativity of the chalcogen decreases.⁸ Further research has found that this increase is due to greater π -electron conjugation to the chalcogen.^{18,19} Since it is known the electron delocalization in amides involves the $n_N \rightarrow \pi^*_{[C-X]}$ transfer, the closer in energy these orbitals are, the greater the overlap is.^{8,20}

Extensive studies have been performed on *N,N*-dimethylacetamide (DMA), *N,N*-dimethylformamide (DMF),^{18,21,22} as well as thioformamides,¹⁸ selenamides,²³ carbamates²⁴ and others^{4,25} to determine the effects of solvent on the rotational barriers. One of the earliest reports on this topic by Drakenberg *et al.* presented an NMR line shape analysis of DMF and DMA in various solvents to determine the barrier. They have found that proton-donating solvents such as H₂O hydrogen bond to the amide oxygen, thereby increasing the rotational barrier by

* E-mail: robinsonr@ukzn.ac.za

ca. 8–12 kJmol⁻¹ (2–3 kcal/mol). Other less polar solvents capable of associating with the amide oxygen have been shown to increase the barrier by ca. 4 kJmol⁻¹ (1 kcal/mol).²² Likewise this indicates that in dilute nonpolar solutions, the natural association that would normally have existed in neat solutions between amide molecules is severed.

More recently, Wiberg *et al.* published a combined experimental and theoretical study on the effect of solvent. In accord with earlier reports, it was found that the barriers of DMA and DMF increased in polar solvents. The reason for this observation being greater stabilization of the ground state as it is more polar than the transition states. However, it was also noted that the effect of solvent on DMA was appreciably larger than DMF. As DMA prefers the anti-TS which has a smaller dipole moment, the difference in stabilization between ground and transition states is thus much greater resulting in an enhanced solvent effect.¹⁸ These effects were coherent with those obtained for *N,N*-dimethylthioformamide (DMTF) and *N,N*-dimethylthioacetamide (DMTA), excepting that the solvent effects on thioamide analogues are significantly larger. The reason for this being the greater difference in dipoles between ground and transition state due to the larger ground state dipole moment of thioamides.¹⁸

Additional investigations on selenoamides have shown that substitution of H at the α -position with a more electronegative or electron withdrawing group results in a decrease in the rotational barrier, while electron donating groups have shown to increase the barrier.^{23,26} This increase is a result of increased resonance through the nitrogen lone pair. However, this is not always the case as shown by Kaur *et al.* with π -donors at the α -position such as NO₂ and CN, as they stabilize the transition states resulting in the observed decrease in the rotational barrier.²³ Also noted in a study of amide resonance in thio- and seleno- carbamates,⁸ the substitution of sulphur for selenium caused an increase in the rotational barrier. This was attributed to the larger size of selenium which in turn causes a decrease in the $n_x \rightarrow \pi^*_{[C-O]}$ transfer and thus less competition for population of the $\pi^*_{[C-O]}$ orbital.

There are various reported methods to experimentally measure the barrier to rotation, among these are; variable temperature NMR,^{27–31} exchange spectroscopy NMR,^{32–35} NMR line shape analysis,^{36,38} pre-saturation³⁹ and computational methods.³ Stemming from previous research performed within our group on the synthesis of various thio and oxo analogues of isopsoralen as potential DNA intercalators, these exhibited varying rotational barriers worthy of further investigation.^{40,41} For this study we have chosen variable temperature and exchange spectroscopy NMR as well as a computational approach to evaluate the influence of an oxygen or sulphur substituent at the α -position of amide and thioamide variants of 2-oxo-2*H*-chromen-7-yl *N,N*-dimethylcarbamate on the rotational barrier.

Variable temperature NMR spectroscopy is used to determine the coalescence temperature of an exchangeable process sufficiently slow at low temperatures to produce distinct signals. As the temperature is increased, a coalescence of these signals is seen to occur until the exchange process is sufficiently fast so as to become indistinguishable by NMR resulting in a single broad signal. Figure 1 shows a characteristic coalescence at 316 K of the two methyl peaks of a dimethylcarbamothioate group.⁴⁰

Once the coalescence temperature, T_c , has been determined, there are two possible techniques to calculate the rotational barrier, ΔG . The first is illustrated by equation 1:

$$\Delta G = 2.303 RT_c (\log k_b T_c / h - \log 2.22 \Delta\nu) \quad (1)$$

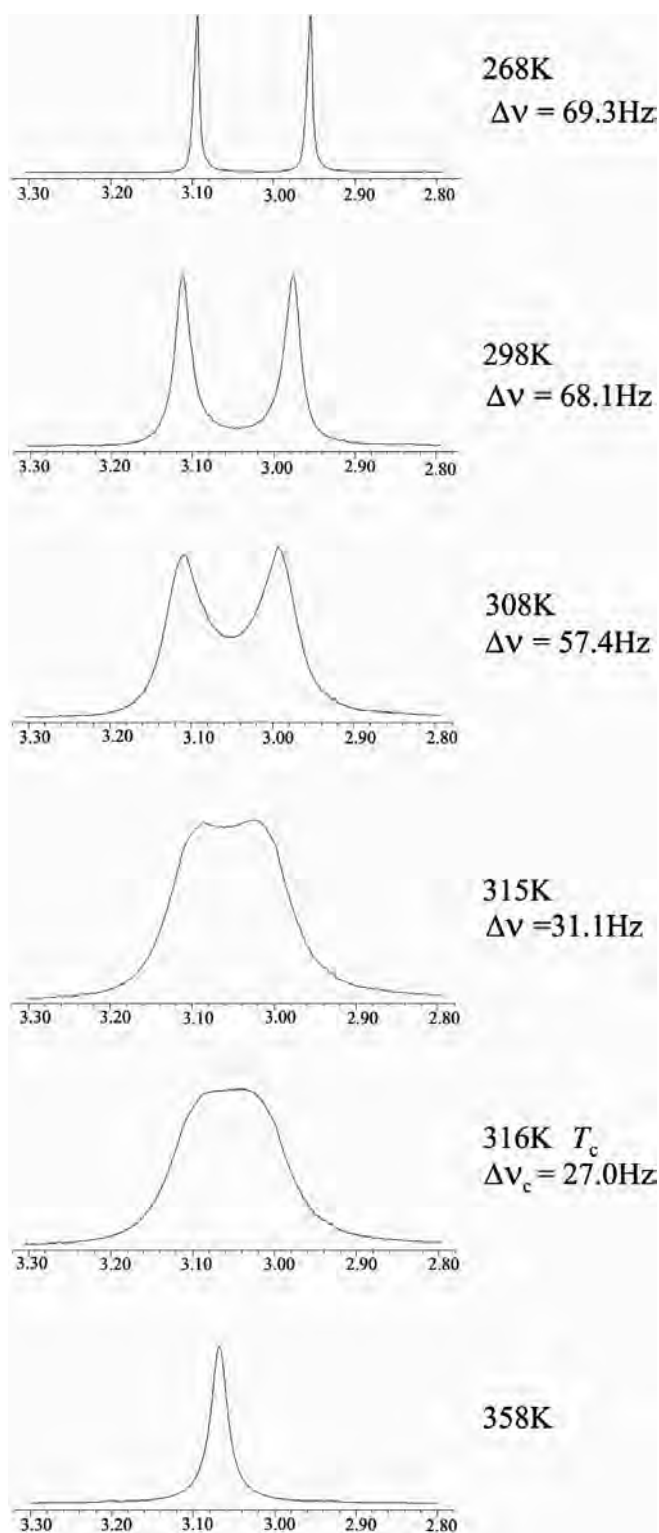


Figure 1 Partial ¹H NMR Spectrum showing coalescence of two methyl peaks of a dimethylcarbamothioate group.⁴⁰

where R = gas constant, T_c = coalescence temperature (K), k_b = Boltzmann's constant, h = Planck's constant, $\Delta\nu$ = difference in chemical shift when signals are completely resolved (Hz).

The other method as reported by Smith *et al.*²⁸ makes use of $\Delta\nu_c$, the estimated difference in chemical shift at the coalescence point, and is calculated as follows:

$$\Delta G = RT_c [22.96 + \ln (T_c / \Delta\nu_c)] \quad (2)$$

Although theoretically similar, in practice Equation 1 is prefer-

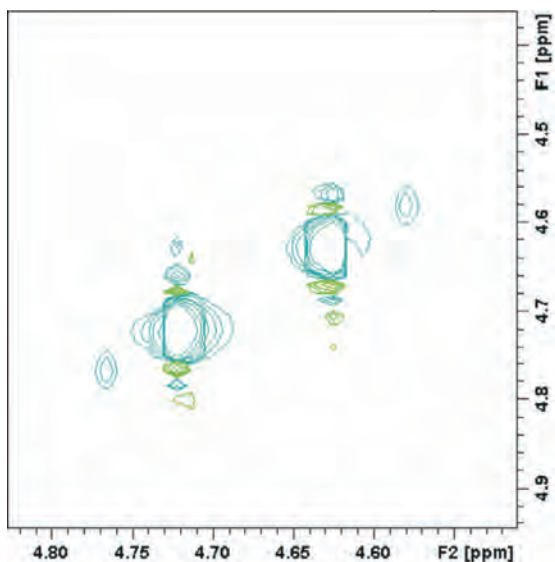


Figure 2 Partial ^1H 2D NOESY's showing the two methyl peaks of a dimethylcarbamothioate group at mixing times of (a) 0 ms (left) and (b) 1147 ms (right).

able as it becomes indeterminate where exactly the 'correct' coalescence occurs and additionally difficult to determine $\Delta\nu_c$ if the signals have coalesced.

Exchange spectroscopy is a 2D NOESY method, which makes use of two spectra, one taken with no mixing time and one taken with a mixing time large enough for the magnetization exchange process to take place. A typical example is shown in Fig. 2.

Using the intensities of the relevant peaks, it is possible to quantitatively calculate the magnetization exchange rates of the exchange equilibrium (k'), which is related to the rate constants of the reaction (k). This is achieved using the EXSYCalc program.⁴² In turn, the rate constant is used to calculate the rotational barrier from the Eyring equation:

$$\Delta G = -RT \ln(k_1h/k_bT), \quad (3)$$

where, R = gas constant, h = Planck's constant, k_b = Boltzmann's constant, T = temperature at the spectra were recorded (K), k_1 = reaction rate constant.

The purpose of the zero mixing time experiment is as a reference.

2. Results and Discussion

A range of carbamates were synthesized as previously described,⁴³ (see Fig. 3) and the three techniques were employed

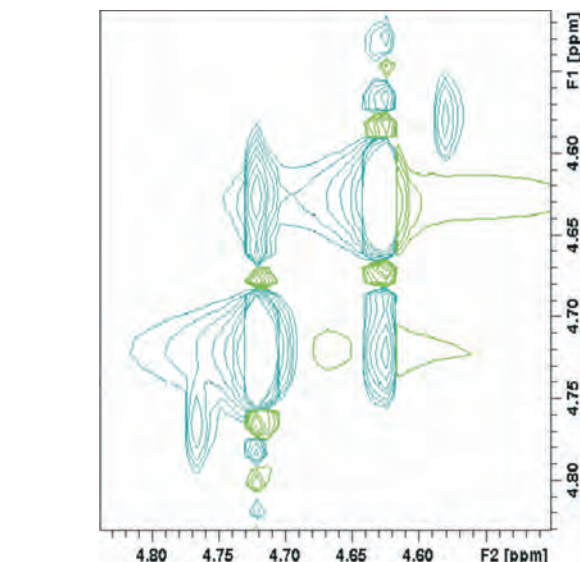
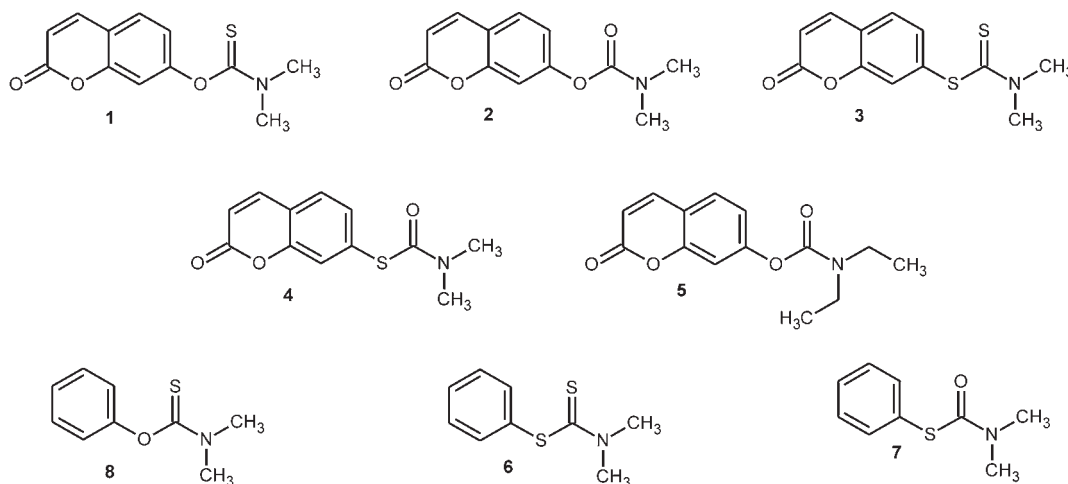


Figure 3 Carbamate compounds investigated

to investigate and contrast their amide rotational barriers.

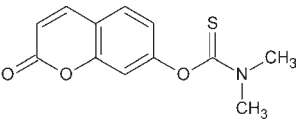
For ease of discussion, the following analysis methods are discussed only for compound **1** shown above. Raw data sets obtained for this compound from each technique are shown in Table 1.

Variable temperature NMR was carried out in deuterated 1,1,2,2-tetrachloroethane to accommodate the wide temperature range required for this study. The barrier to rotation was then calculated using Equation 1.

Exchange spectroscopy (EXSY) was chosen for comparison of results with those obtained by variable temperature, as well as to evaluate this fairly new technique as a reliable method to calculate rotational barriers. As solvent plays an effect on the rotational barrier,^{18,21,22} the same solvent was selected as for the variable temperature study, namely deuterated 1,1,2,2-tetrachloroethane, to exclude variations in the solvent effect. The absolute integrals of the amide methyl and cross peak areas were quantified and using the EXSYCalc program to yield the chemical exchange rate constants. This value was then substituted into the Eyring equation to calculate the rotational barrier, $\Delta_{rot}G$.

To evaluate ΔG from computational data, first the structure of each compound was optimized to a ground state, from which a 360° scan of the $\text{X}=\text{C}-\text{N}-\text{CH}_3$ dihedral was performed. Following this rotation profile, two transition states were identified: where the nitrogen lone pair and carbonyl heteroatom are respectively syn or anti to one another. To avoid unnecessary

Table 1 Raw data used to calculate ΔG obtained from each method.

| Structure | Raw data | | | | |
|---|----------------|-------------------------------------|--------------------------------|----------------------------|----------------------------|
|  | EXSY | K_1 | $\Delta_{rot}G/kJmol^{-1}$ | K_{-1} | $\Delta_{rot}G/kJmol^{-1}$ |
| | | 1.513 | 72.00 | 0.027 | 81.98 |
| | Variable temp. | T_i/K | ν/Hz | $\Delta_{rot}G/kJmol^{-1}$ | |
| | | 39.3 | 46.70 | 82.01 | |
| | Computational | $\Delta_{rot}G_{syn-ts}/kJmol^{-1}$ | $\Delta G_{syn-ts}/kJmol^{-1}$ | | |
| | | 82.41 | 78.18 | | |

calculations, it was assumed that the most stable conformation with respect to rotation about the α -position would be where the coumarin system and amide moiety are perpendicular to one another (Fig. 4). This was tested in one complex at the ground state and supported the above assumption.

It was found that the higher energy transition state was that of the syn conformer ($+4.22 \text{ kJ mol}^{-1}$), correlating to electronic repulsion between the nitrogen lone pair and applicable chalcogen. Frequency calculations performed on the geometry optimized transition states exhibited a single imaginary vibration corresponding to amine rotation away from the amide chalcogen. This verifies they are indeed true transition states of the rotation.

In order to obtain the rotational barrier for each molecule, frequency data was obtained for all optimized ground and transition states, and the following equation was used:⁴⁴

$$\Delta_{rot}G = \Delta G_{\text{transition state}}(298 \text{ K}) - \Delta G_{\text{ground state}}(298 \text{ K}) .$$

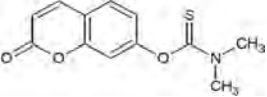
However, since the computational output only provides the sum of electronic and thermal energies, this equation transforms as follows:

$$\Delta_{rot}G (298 \text{ K}) = (\epsilon_0 + G_{\text{corr}})_{\text{transition state}} - (\epsilon_0 + G_{\text{corr}})_{\text{ground state}} ,$$

where, ϵ_0 is the total electronic energy. In this way two rotational barriers are obtained, each corresponding to rotation through their respective transition states. Similarly, it is possible to calculate $\Delta_{rot}H$ and $\Delta_{rot}S$.

Looking at the variation in bond length with amide rotation, it is seen that the C=S bond varies very little on rotation with the key changes occurring in the C-N bond. These changes are

Table 2 Selected changes in bond lengths for the two calculated transition states of compound 1. [a] Difference between ground and transition state structures. [b] A negative change in bond length indicates shortening. [c] Calculated DFT data.

| Structure | Bond length change a,b,c/Å | | |
|--|----------------------------|----------|---------|
| | O-C | C=S | C-N |
|  | | | |
| Syn-transition state | -0.00342 | -0.03188 | -0.0627 |
| Anti-transition state | -0.0182 | -0.02284 | 0.06811 |
| Ground state | 1.432 | 1.666 | 1.356 |

shown in Table 4 and graphically illustrated in Fig. 5.

From Fig. 5, we see that the C-O bond is almost completely unaffected by rotation. The C=S bond is also essentially unaffected with only a slight decrease in bond length compared to the large increase in the length of C-N. Numerical values are shown in Table 2.

The C=S bond decreases by 0.02–0.03 Å, where the C-N bond lengthens by a larger 0.06–0.07 Å, clearly indicating the main participants in this electron delocalization are the carbonyl carbon and nitrogen atoms. These results are consistent with those obtained by Wiberg *et al.*¹⁴ and likewise contradict Pauling's classical model of resonance. Interesting to note is that C-O bond length decreases more in the anti-TS while the C=S bond length shortens in the syn-TS. This suggests that there is

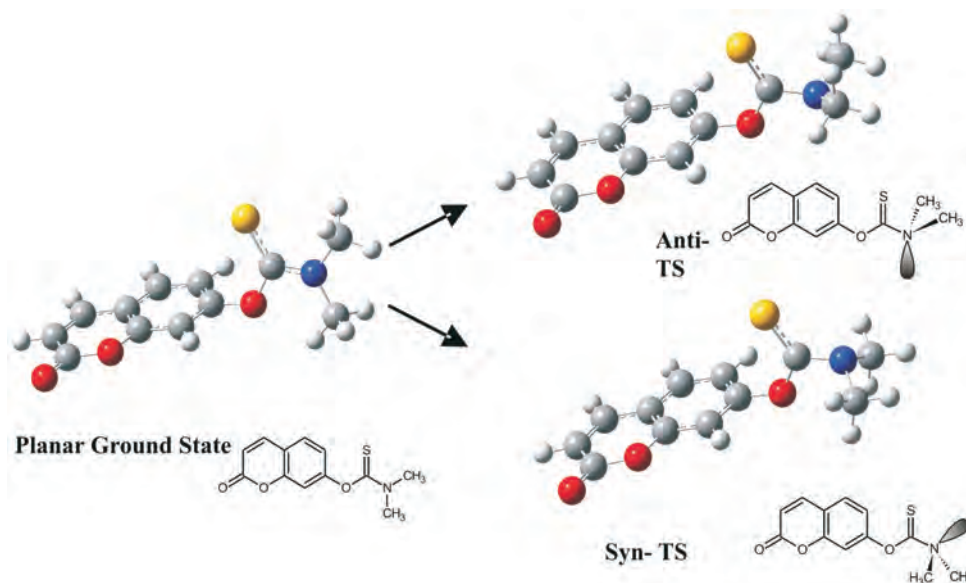
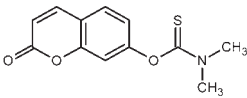
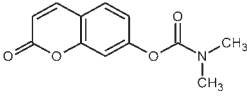
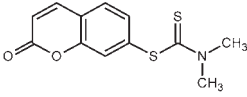
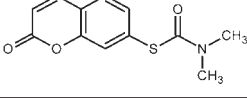
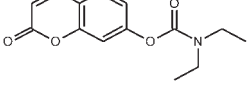
**Figure 4** The syn- and anti-transition states [B3LYP/6-31+G(d)].

Table 3 Free energies of rotation for coumarin analogues. [a] Variable Temperature results obtained from previous work within our group⁴⁰ [b] All EXSY data collected as 30°C.

| Entry | Carbamate | Variable temperature NMR ^a | Exchange spectroscopy NMR ^b | Computational data |
|-------|---|---------------------------------------|--|--|
| 1 |  | $\Delta G = 82.01 \text{ kJmol}^{-1}$ | $\Delta G = 81.98 \text{ kJmol}^{-1}$ | $\Delta G_{\text{anti-TS}} = 78.10 \text{ kJmol}^{-1}$ |
| 2 |  | $\Delta G = 71.35 \text{ kJmol}^{-1}$ | $\Delta G = 75.01 \text{ kJmol}^{-1}$ | $\Delta G_{\text{anti-TS}} = 74.52 \text{ kJmol}^{-1}$ |
| 3 |  | $\Delta G = 69.75 \text{ kJmol}^{-1}$ | — | $\Delta G_{\text{anti-TS}} = 59.33 \text{ kJmol}^{-1}$ |
| 4 |  | $\Delta G = 64.61 \text{ kJmol}^{-1}$ | $\Delta G = 63.52 \text{ kJmol}^{-1}$ | $\Delta G_{\text{anti-TS}} = 58.79 \text{ kJmol}^{-1}$ |
| 5 |  | — | $\Delta G = 83.99 \text{ kJmol}^{-1}$ | $\Delta G_{\text{anti-TS}} = 84.07 \text{ kJmol}^{-1}$ |

greater $n_{\text{O}} \rightarrow \pi^*_{[\text{C}=\text{S}]}$ transfer in the syn-TS, whereas there is greater $n_{\text{N}} \rightarrow \pi^*_{[\text{C}=\text{S}]}$ transfer in the anti-TS. This same trend is observed for all the compounds investigated.

Since there is a preference for rotation through the lower energy anti-TS, these were the computationally obtained values used to be a more accurate representation of the measured quantities, although in reality, the latter is undoubtedly larger due to a statistical mixture of rotation through both transition states.

Comparative data is shown in Tables 3 and 4. As can be seen, the NMR and computational methods are in excellent agreement with one another. As the molecular calculations were performed in the gas phase, the experimental values are on the whole larger due to solvent and other interactive molecular effects.

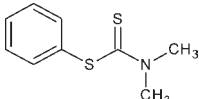
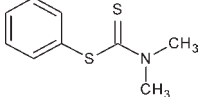
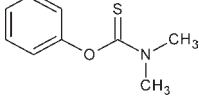
Consistent with previous reports,^{1,17,4–47} thioamides **1** and **3(6)** have a substantially larger barrier to rotation than their respective amides **2** and **4**; however, the presence of α -sulphur (as opposed to oxygen) decreases the magnitude of this difference

to virtually zero. Significant is the decrease in barrier with replacement of oxygen at the α -position with sulphur, consistent with earlier results that the rotational barrier is due to $n_{\text{N}} \rightarrow \pi^*_{[\text{C}=\text{X}]}$ electron transfer.^{8,20,23} Also, substitution of the methyl groups for ethyl's (entries **2** and **5**) shows a significant increase in the rotational barrier. This increase is due to the larger inductive effect of CH_3CH_2- as compared to CH_3- , conceivably resulting in enhancement of $n_{\text{N}} \rightarrow \pi^*_{[\text{C}=\text{X}]}$ electron transfer. This is consistent with early reports that substituents on the nitrogen produced the opposite effect on the rotational barrier than if they were on the carbonyl.⁴⁸

Due to problems experienced in the synthesis of the dithiol derivative (complex **3** in Fig. 3, entry 3 in Table 3), a study was carried out using analogues derived from phenol and thiophenol.⁴³ This data is presented in Table 4.

Phenol derivative **8** is in excellent agreement with its coumarin equivalent, **1**, likewise for compounds **7** and **4**. Thus, we have established that the phenol derivatives are satisfactory equiva-

Table 4 Free energies of rotation for phenol analogues. [a] All EXSY data acquired at 30 °C unless otherwise indicated. [b] Data acquired at –15 °C as the amide methyl signals were either completely or partially coalesced at ambient temperature.

| Entry | Carbamate | Variable temperature NMR ^a | Exchange spectroscopy NMR ^b | Computational data |
|-------|---|---------------------------------------|--|--|
| 6 |  | — | $\Delta G = 59.38 \text{ kJmol}^{-1}$ | $\Delta G_{\text{anti-TS}} = 56.58 \text{ kJmol}^{-1}$ |
| 7 |  | — | $\Delta G = 59.80 \text{ kJmol}^{-1}$ | $\Delta G_{\text{anti-TS}} = 59.41 \text{ kJmol}^{-1}$ |
| 8 |  | — | $\Delta G = 79.97 \text{ kJmol}^{-1}$ | $\Delta G_{\text{anti-TS}} = 76.31 \text{ kJmol}^{-1}$ |

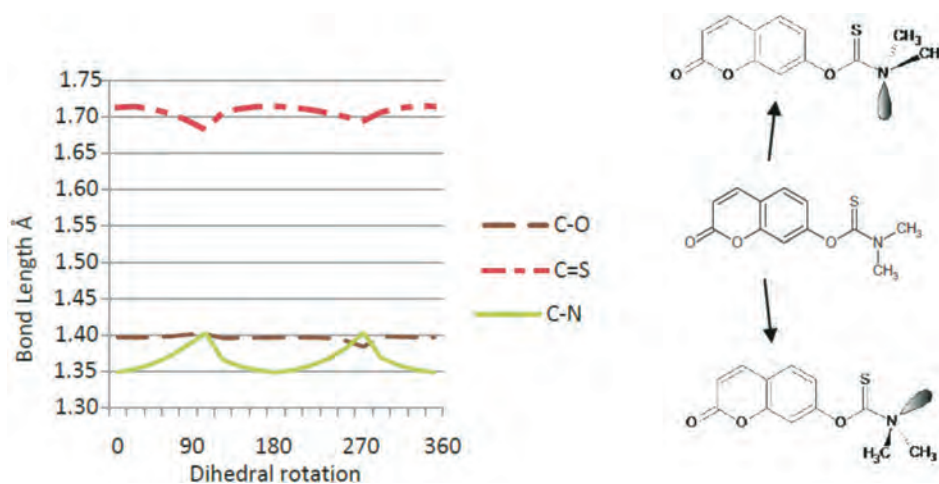


Figure 5 Typical Variation of the Calculated Bond Length (Å) with dihedral rotation through 360° [B3LYP/6-31+G(d)].

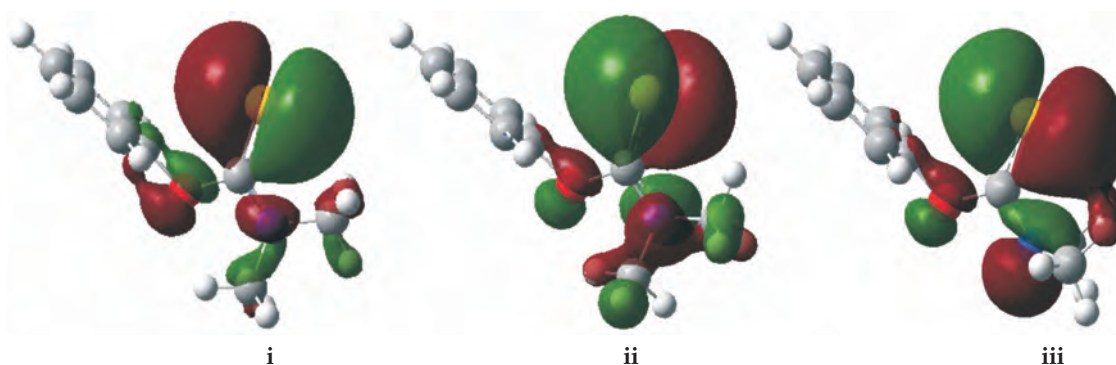


Figure 6 HOMO of (i) ground state, (ii) dihedral rotation through 40° and (iii) anti-TS of O-phenol *N,N*-dimethylcarbamothioate.

Table 5 Comparison of bond lengths (Å).

| Bond | Computational | X-ray diffraction | Literature ^a |
|------|---------------|-------------------|-------------------------|
| C-S | 1.822 | 1.788 | 1.82 (single) |
| C=S | 1.666 | 1.661 | 1.56 (double) |
| C-n | 1.356 | 1.336 | 1.34 (partial double) |

^a Literature values taken from ref. 49.

lents for the coumarin analogues, and the value obtained for **6** may be used as an adequate approximate value for compound **3**.

Examination of the HOMO's (Fig. 6) for both the ground state and anti-transition state, shows the carbonyl (or thiocarbonyl) orbitals unchanged between ground state and rotated transition state. This applies as well to the lone pairs of the atom in the α -position. On the nitrogen, however, we see a large increase in the orbital density in the transition state and in the slightly rotated form, indicating that the lone pair is 'regained' on rotation away from the planar ground state.

These observations of the HOMO orbitals correlate with the bond length data, supporting the model by Wiberg *et al.* that the carbonyl (or thiocarbonyl), is effectively a spectator to rotation about the amide bond.

X-ray diffraction analysis of compound **6** (Fig. 7) shows the molecules to align in a $P2_1/c$ space group. Bond angles and lengths correlate favourably to the computational data obtained for the ground state, reflecting the partial double bond character along the C-N bond.

Table 5 shows the bond lengths for the ground state of compound **6** as obtained computationally and from the X-ray

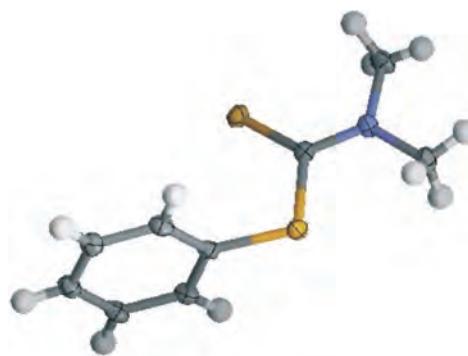


Figure 7 ORTEP model from crystal structure of compound **6**.

structure analysis. To our delight, the two data sets correlate exceedingly well both with one another and with literature values.

The crystal structure reflects the ground state of the molecule where the carbamate group is *ca.* 90° to the phenyl ring and the amide grouping is planar, indicating our initial assumption that this would be the most stable position with regard to rotation about the -S-C- bond at the α -position was sound.

4. Conclusions

The eight compounds previously synthesized⁴³ were analyzed by variable temperature and exchange spectroscopy NMR to determine the barrier to internal rotation in these α -substituted amides. These barriers were also determined computationally, and all methods were found to be in excellent agreement, and we can conclude that EXSY NMR is a reliable technique to

evaluate rotational barriers, and additionally as a time saving equivalent to variable temperature NMR. The crystal structure of **6** correlates with the computational data obtained, and adds significance to computational methods as applied within this study. All the results obtained verify the model proposed by Wiberg *et al.*, not to say that Pauling's model is incorrect, but merely insufficient to describe adequately the factors involved in amide resonance.

5. Experimental

X-Ray Crystallography

Crystallographic measurements were made using a 3 kW Spellman X-ray generator with a 3 kW ceramic X-ray tube and an Xcalibur 2 CCD diffractometer. The structure was solved using the SHELXS-97⁵⁰ program by direct methods. The structure was plotted using the program ORTEP⁵¹

Crystal Data of Compound 6. C₉H₁₁NS₂, *M* = 197.31, *T* = 100(2) K, λ = 0.71073 Å, *a* = 7.538(5), *b* = 8.989(5), *c* = 14.229(5) Å, α = 90.000(5), β = 90.959(5), γ = 90.000(5), *V* = 964.0(9) Å³, space group *P*2₁/*c*, *Z* = 4, *D*_x = 1.359 mg m⁻³, μ = 0.495 mm⁻¹, *F*(000) = 416. Crystal size 0.6 × 0.55 × 0.25 mm; θ range for data collection 3.82–34.11; index range -10 < *h* < 11, -13 < *k* < 13, -21 < *l* < 21; reflections collected 14324; independent reflections 3567 [*R*_{int}] = 0.0538; refinement method full-matrix least-squares on *F*²; data/restraints/parameters 3567:0:153; goodness-of-fit on *F*² 1.071; *R*(*F*) [*I* > 2 σ (*I*)] = 0.0568; *wR*₂ = 0.1461; largest diff. peak and hole 1.721 and -0.986 e Å⁻³. CCDC-711835 contains the supplementary crystallographic data for this paper. These data can be obtained free of charge from The Cambridge Crystallographic Data Centre via www.ccdc.cam.ac.uk/data_request/cif.

EXSY Data Collection

Exchange spectroscopy (EXSY) data were collected at 30°C in 1,1,2,2-tetrachloroethane. The absolute integrals of the amide methyl groups as well as the cross peaks were recorded for two experiment with mixing times of 0 and *x* (where *x* was large enough for the exchange process to occur, and was typically of the order of 1000 ms). The intensities of the methyl groups and cross peaks were entered into the EXSYCalc program,⁵² which calculated the chemical exchange rate constants. The chemical exchange rate constant was substituted into the Eyring equation in order to calculate $\Delta_{\text{rot}}G$.

Computational Details

All *ab initio* gas phase calculations were performed using the Gaussian 03W package⁵³ at the DFT (B3LYP) level of theory with the 6-31+G(d) basis set. In this case, the diffuse functions were incorporated in order for a more accurate description of π -electron delocalization and the lone pairs associated with oxygen, sulphur and nitrogen. The ground state geometries of all amide compounds were optimized, following a scan calculation in which the amide dihedral angle was rotated. The structures associated with the two maxima on the energy profile of the scan were manually extracted and used as starting structures in a full transition state optimization (no constraints) at the same level of theory and basis set. Each of the two possible transition states had one negative eigenvalue only. Analysis of the movement of atoms associated with this eigenvalue confirmed rotation of the amide bond, as expected for these transition states. Thermochemical data was obtained from frequency calculations performed on both ground and transition states.

Cartesian coordinates of all geometry optimized structures are available as supplementary material.

References

- 1 K.E. Laidig and L.M. Cameron, *J. Am. Chem. Soc.*, 1996, **118**, 1737–1742
- 2 C.R. Kemnitz and M.J. Loewen, *J. Am. Chem. Soc.*, 2007, **129**, 2521–2528.
- 3 J.S. Craw, I.H. Hillier, G.A. Morris and M.A. Vincent, *Mol. Phys.*, 1997, **92**, 421.
- 4 F.J. Luque and M. Orozco, *J. Chem. Soc., Perkin Trans. 2*, 1993, 683–690.
- 5 H. Lee, M. Lee, Y. Choi, H. Park and K. Lee, *J. Mol. Struct.: THEOCHEM*, 2003, **631**, 101.
- 6 H. Basch and S. Hoz, *Chemical Physics Letters*, 1998, **294**, 117.
- 7 R.N. Salvatore, F. Chu, A.S. Nagale, E.A. Kapxhiu, R.M. Cross and K.W. Jung, *Tetrahedron*, 2002, **58**, 3329–3347.
- 8 D. Kaur, *J. Mol. Struct.: THEOCHEM*, 2005, **757**, 149–153.
- 9 J.H. Wynne, S.D. Jensen and A.W. Snow, *J. Org. Chem.*, 2003, **68**, 3733–3735.
- 10 M. Koketsu, Y. Fukuta and H. Ishihara, *J. Org. Chem.*, 2002, **67**, 1008–1011.
- 11 M. Feroci, M.A. Casadei, M. Orsini, L. Palombi and A. Inesi, *J. Org. Chem.*, 2003, **68**, 1548–1551.
- 12 F.J. Luque and M. Orozco, *J. Chem. Soc. Perkin Trans. 2*, 1993, 683–690.
- 13 L. Pauling, *Proc. R. Soc. Lond. A*, 1977, **356**, 433–441.
- 14 K.B. Wiberg and K.E. Laidig, *J. Am. Chem. Soc.*, 1987, **109**, 5935–5943.
- 15 K.B. Wiberg and C.M. Breneman, *J. Am. Chem. Soc.*, 1992, **114**, 831–840.
- 16 K.B. Wiberg and R. Glaser, *J. Am. Chem. Soc.*, 1992, **114**, 841–850.
- 17 K.B. Wiberg and P.R. Rablen, *J. Am. Chem. Soc.*, 1995, **117**, 2201–2209.
- 18 K.B. Wiberg and D.J. Rush, *J. Am. Chem. Soc.*, 2001, **123**, 2038.
- 19 D. Lauvergnat and P.C. Hiberty, *J. Am. Chem. Soc.*, 1997, **119**, 9478–9482.
- 20 P.V. Bharatam, R. Moudgil and D. Kaur, *J. Phys. Chem. A*, 2003, **107**, 1627–1634.
- 21 K.B. Wiberg, P.R. Rablen, D.J. Rush and T.A. Keith, *J. Am. Chem. Soc.*, 1995, **117**, 4261.
- 22 T. Drakenberg, K. Dahlqvist and S. Forsen, *J. Phys. Chem.*, 1972, **76**, 2178.
- 23 D. Kaur, P. Sharma, P.V. Bharatam and N. Dogra, *J. Mol. Struct.: THEOCHEM*, 2006, **759**, 41–49.
- 24 C. Cox, T. Lectka, *J. Org. Chem.*, 1998, **63**, 2426.
- 25 Y. Otani, O. Nagae, Y. Naruse, S. Inagaki, M. Ohno, K. Yamaguchi, G. Yamamoto, M. Uchiyama, T. Ohwada, *J. Am. Chem. Soc.*, 2003, **125**, 15191–15199.
- 26 B. Galabov, S. Ilieva, B. Hadjieva, E. Dinchova, *J. Phys. Chem. A*, 2003, **107**, 5854–5861.
- 27 C. Piccinni-Leopardi, O. Fabre, D. Zimmermann and J. Reisse, *Can. J. Chem.*, 1977, **55**, 2649–2655.
- 28 R.J. Smith, D.H. Williams and K. James, *Chem. Commun.*, 1989, 682–683.
- 29 E.A. Basso, P.R. Oliveira, F. Wietzycoski, R.M. Pontes and B.C. Fiorin, *J. Mol. Struct.* 2005, **753**, 139–146.
- 30 D.G. Gehring, W.A. Mosher and G.S. Reddy, *J. Org. Chem.*, 1966, **31**, 3436–3437.
- 31 D. Kost and H. Egozy, *Journal of Organic Chemistry, The*, 1989, **54**, 4909.
- 32 B.J. Wik, M. Lersch, A. Krivokapic and M. Tilset, *J. Am. Chem. Soc.*, 2006, **128**, 2682–2696.
- 33 A. Anand, A.D. Roy, R. Chakrabarty, A.K. Saxena and R. Roy, *Tetrahedron*, 2007, **63**, 5236–5243.
- 34 T. Ayama, H. Sakane, T. Muneishi and T. Hirao, *Chem. Commun.*, 2008, 765–767.
- 35 I. Pianet and J.M. Vincent, *Inorg. Chem.*, 2004, **43**, 2947–2953.
- 36 H.C. Bushweller, J.W. O'Neil, M.H. Halford and F.H. Bissett, *J. Am. Chem. Soc.*, 1971, **93**, 1471–1473.
- 37 S.A. Matchett, G. Zhang and D. Frattarelli, *Organometallics*, 2004, **23**, 5440–5449.
- 38 R. Singh and G.M. Whitesides, *J. Am. Chem. Soc.*, 1990, **112**, 1190–1197.
- 39 R. Quintanilla-Licea, J.F. Colunga-Valladares, A. Caballero-Quintero, C. Rodriguez-Padilla, R. Tamez-Guerra, R. Gomez-Flores and N. Waksman, *Molecules*, 2002, **7**, 662–673.

- 40 D.J. Clarke, *Synthetic and Spectroscopic Studies of Isopsoralen Derivatives*, M.Sc. thesis, University of Natal, Pietermaritzburg, South Africa, 2001.
- 41 D.J. Clarke and R.S. Robinson, *Tetrahedron*, 2002, **58**, 2831–2837.
- 42 J.C. Cobas and M. Martin-Pastor, *MestReC*, 2004.
- 43 C.K.A. Janse van Rensburg and R.S. Robinson, *S. Afr. J. Chem.*, 2009, **62**, 143–148.
- 44 J.W. Ochterski, in http://www.gaussian.com/g_whitepap/white_pap.htm, 2000.
- 45 E.D. Glendening and J.A. Hrabal, *J. Am. Chem. Soc.*, 1997, **119**, 12940–12946.
- 46 N.G. Vassilev and V.S. Dimitrov, *J. Mol. Struct.*, 2003, **654**, 27–34.
- 47 Y. Mo, P. von Rague Schleyer, W. Wu, M. Lin and Q. Zhang, *J. Gao, J. Phys. Chem. A*, 2003, **107**, 10011–10018.
- 48 C.H. Yoder and R.D. Gardner, *J. Org. Chem.*, 1981, **46**, 64–66.
- 49 R.C. Weast, *Handbook of Chemistry and Physics*, 63rd Edn; Boca Raton: Florida, 1984.
- 50 G.M. Sheldrick, in *SHELXS-97, Program for Solution of Crystal Structures*, University of Gottingen, Germany, 1997.
- 51 L.J. Farrugia, In *ORTEP 3 for Windows, V1.01 beta*, Department of Chemistry, University of Glasgow, Scotland, 1998.
- 52 EXSYCalc, is available for free download from Mestrelab research.
- 53 Gaussian 03, Version 6.0, M.J. Frisch, G.W. Trucks, H.B. Schlegel, G.E. Scuseria, M.A. Robb, J.R. Cheeseman, J.A. Montgomery, Jr., T. Vreven, K.N. Kudin, J.C. Burant, J.M. Millam, S.S. Iyengar, J. Tomasi, V. Barone, B. Mennucci, M. Cossi, G. Scalmani, N. Rega, G.A. Petersson, H. Nakatsuji, M. Hada, M. Ehara, K. Toyota, R. Fukuda, J. Hasegawa, M. Ishida, T. Nakajima, Y. Honda, O. Kitao, H. Nakai, M. Klene, X. Li, J.E. Knox, H.P. Hratchian, J.B. Cross, C. Adamo, J. Jaramillo, R. Gomperts, R.E. Stratmann, O. Yazyev, A.J. Austin, R. Cammi, C. Pomelli, J.W. Ochterski, P.Y. Ayala, K. Morokuma, G.A. Voth, P. Salvador, J.J. Dannenberg, V.G. Zakrzewski, S. Dapprich, A.D. Daniels, M.C. Strain, O. Farkas, D.K. Malick, A.D. Rabuck, K. Raghavachari, J.B. Foresman, J.V. Ortiz, Q. Cui, A.G. Baboul, S. Clifford, J. Cioslowski, B.B. Stefanov, G. Liu, A. Liashenko, P. Piskorz, I. Komaromi, R.L. Martin, D.J. Fox, T. Keith, M.A. Al-Laham, C.Y. Peng, A. Nanayakkara, M. Challacombe, P.M.W. Gill, B. Johnson, W. Chen, M.W. Wong, C. Gonzalez and J.A. Pople, Gaussian, Inc., Pittsburgh.